Singlet−Triplet Gaps and Spin Potentials

Rubicelia Vargas, Marcelo Galván, and Alberto Vela*

Departamento de Química División de Ciencias Básicas e Ingeniería Universidad Autónoma Metropolitana-Iztapalapa A.P. 55-534, México, Distrito Federal 09340, Mexico

Received: September 12, 1997; In Final Form: February 13, 1998

The relation between vertical and adiabatic singlet−triplet gaps and the generalized spin-dependent global response coefficients is presented. Local, semilocal, and hybrid density functional calculations of these quantities for the halocarbenes CXY, where X and Y are H, F, Cl, Br, and I, show that the vertical gaps are better reproduced at the local level. Hybrid functionals overestimate them considerably. For the whole series of halocarbenes considered, except CHI, calculations predict the singlet $^1A_1$ as the ground state. The only exception found is for the hybrid calculation of CHI that predicts $^3B_1$ as the ground state for this halocarbene. For all functionals, there is a linear relation between the vertical singlet−triplet energy gap and the spin potential (the first derivative of the total energy with respect to the number of unpaired electrons), and the inclusion of the spin hardness (the second derivative of the total energy with respect to the number of unpaired electrons) improves this relationship considerably. It is also shown that the geometrical relaxation accompanying the adiabatic excitation in the halocarbenes is constant.

I. Introduction

Several recent works have shown that the spin-polarized extension of density functional theory (DFT) broadens the capabilities of this approach to chemical reactivity. Galván et al.[1] have presented the general formalism in a representation where the independent variables are the total number of electrons (N) and the number of unpaired electrons (N_S). Later, Galván and Vargas applied the formalism to atoms showing that some of these global coefficients have a periodic behavior[2] and established the connection between the generalized spin-polarized Fukui functions and Hund's rule.[3] The spin-polarized extension of chemical reactivity can also be developed in a representation where the independent variables are the number of spin $\alpha(N_\uparrow)$ and spin $\beta(N_\downarrow)$ electrons. These variables are related to N and N_S by the expressions $N = N_\uparrow + N_\downarrow$ and $N_S = N_\uparrow - N_\downarrow$. Using this latter representation, Ghanty and Ghosh[4−8] showed, for the first time, that the spin-polarized extension of the DFT approach to chemical reactivity leads to a solid theoretical justification of one of the landmark expressions in chemistry: Pauling's covalent contribution to bond energies.

In the $\{N, N_S\}$ representation, the total energy of a system can be expanded in a Taylor series around a reference ground state with N^0 electrons, with N_S^0 unpaired electrons, and in the presence of an external potential $v^0(\mathbf{r})$ as

$$\Delta E \cong E[N,N_S,v(\mathbf{r})] - E[N^0,N_S{}^0,v^0(\mathbf{r})]$$

$$= \mu_N^0\Delta N + \mu_S^0\Delta N_S + \int d\mathbf{r}\, \rho^0(\mathbf{r})\, \Delta v(\mathbf{r}) + {}^1/_2\eta_{NN}^0(\Delta N)^2 + \eta_{NS}^0\Delta N\Delta N_S + {}^1/_2\eta_{SS}^0(\Delta N_S)^2 + \Delta N\int d\mathbf{r}\, f_N{}^0(\mathbf{r})\, \Delta v(\mathbf{r}) + \Delta N_S\int d\mathbf{r}\, f_S{}^0(\mathbf{r})\, \Delta v(\mathbf{r}) + {}^1/_2\int\int d\mathbf{r}\, d\mathbf{r}'\, \chi^0(\mathbf{r},\mathbf{r}')\, \Delta v(\mathbf{r})\, \Delta v(\mathbf{r}') + ... \quad (1)$$

where μ_N is the chemical potential that parallels but is not equal to the usual spin-restricted chemical potential;[2] μ_S, the rate of change of the total energy with respect to the number of unpaired electrons, has been named the spin potential[1] and gauges the tendency of the system to change its spin polarization; η_{NN}, η_{NS}, and η_{SS}, the generalized hardnesses,[1] are the full set of second partial derivatives of the total energy with respect to N and N_S, while $f_N(\mathbf{r})$ and $f_S(\mathbf{r})$ are the generalized Fukui functions[1] corresponding to the first partial derivatives of the electron density $\rho(\mathbf{r})$ with respect to N and N_S, respectively; and, finally, $\chi(\mathbf{r},\mathbf{r}')$ is the linear response function. In deriving eq 1, it has been assumed that the energy functional is such that the order of partial and/or functional derivation is immaterial. The upper index 0 indicates that all of these global and local response functions are evaluated at the reference point.

If one is interested in energy changes that occur at a constant number of electrons, eq 1 reduces to

$$E[N^0,N_S,v(\mathbf{r})] - E[N^0,N_S^0,v^0(\mathbf{r})] \cong \mu_S^0\Delta N_S + \int d\mathbf{r}\, \rho^0(\mathbf{r})\, \Delta v(\mathbf{r}) + {}^1/_2\eta_{SS}^0(\Delta N_S)^2 + \Delta N_S\int d\mathbf{r}\, f_S^0(\mathbf{r})\, \Delta v(\mathbf{r}) + {}^1/_2\int\int d\mathbf{r}\, d\mathbf{r}'\, \chi^0(\mathbf{r},\mathbf{r}')\, \Delta v(\mathbf{r})\, \Delta v(\mathbf{r}') + ... \quad (2)$$

One of the purposes of this work is to analyze the capability of eq 2 to describe energy changes when the total number of electrons is kept fixed while the system suffers a change in the total number of unpaired electrons. An interesting and challenging problem where these types of processes are relevant is the study of the multiplicity changes that occur in halocarbenes. Consequently, the main objective of the present work is to gain some physical and chemical insight on the role played by the spin-dependent global response coefficient in the description of the singlet−triplet energy differences of these chemical systems. The chemistry of these systems has been widely studied.[9−35] It is now well-established that the ground state of halocarbenes can be a singlet or triplet and also that the reactivity of these species is highly dependent on its ground-state

S1089-5639(97)02984-8 CCC: $15.00
Published on Web 04/14/1998

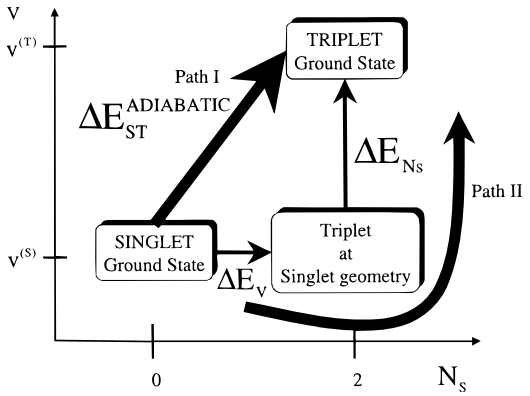

Figure 1. Schematic representation of integration paths in the $\{N_S,v\}$ plane for the calculation of singlet−triplet energy differences. See text for explanation of all quantities.

multiplicity:[36] singlet ground-state carbenes react in one step while triplets are usually involved in a two-stage radical reaction. Experimental determination of the ground-state multiplicity of these systems is limited, and thus, in recent years, several theoretical groups have devoted special attention to the accurate calculation of geometries, frequencies, and singlet−triplet energy gaps of halocarbenes.[16−31] These works reveal that electron correlation is a crucial factor in correctly predicting the relative stability between the singlet and the triplet. The structure of this work is the following. In section II a set of approximations will be used to simplify eq 2. Results corresponding to the calculation of the vertical and adiabatic singlet−triplet energy gaps of halocarbenes using several approximations to the exchange-correlation energy functional (local, semilocal, and hybrid) are presented in section III (computational details can be found in the Appendix). The relation between these energy gaps and the spin potential are discussed in section IV. Conclusions are contained in the last section (V).

II. Approximations to the Spin Potential and Spin Hardness and Their Relation to Vertical and Adiabatic Singlet−Triplet Energy Gaps

The energy differences indicated by eq 2 can be calculated following any continuous path in the $\{N_S,v\}$ plane. However, not only from the conceptual point of view, but also for practical (computational) reasons, the paths depicted in Figure 1 are the most convenient for describing the change from a singlet to a triplet state. To clarify these points, consider a situation where one goes from a singlet ($N_S = 0$) initial state to a triplet ($N_S = 2$) final state. The straightforward way to obtain the energy difference between these two states is to move along path I in Figure 1. In this case, the energy difference corresponds to the adiabatic singlet−triplet energy gap (ΔE_{ST}^{ad}). Using eq 2, one finds that

$$\Delta E_{ST}^{ad} = E[N^0,2,v^{(T)}(\mathbf{r})] - E[N^0,0,v^{(S)}(\mathbf{r})]$$

$$= 2\mu_S^{(S)} + \int d\mathbf{r}\, \rho^{(S)}(\mathbf{r})\, \Delta v(\mathbf{r}) + 2\eta_{SS}^{(S)} + 2\int d\mathbf{r}\, f_S^{(S)}(\mathbf{r}) \times \Delta v(\mathbf{r}) + {}^1/_2 \int\int d\mathbf{r}\, d\mathbf{r}'\, \chi^{(S)}(\mathbf{r},\mathbf{r}')\, \Delta v(\mathbf{r})\, \Delta v(\mathbf{r}') \quad (3)$$

where, as indicated, all response coefficients are evaluated at the singlet (initial) state and $\Delta v(\mathbf{r}) = v^{(T)}(\mathbf{r}) - v^{(S)}(\mathbf{r})$ is the difference between the nuclear potential evaluated at the triplet and singlet ground-state geometries, respectively. Numerically, the evaluation of ΔE_{ST}^{ad} is straightforward: one has to optimize the geometries for the two multiplicities and take the energy difference. An alternative is provided by the right hand side of eq 3. Knowledge of the singlet response coefficients, together with a model for the geometrical relaxation associated with the transition, allows one to estimate the adiabatic singlet−triplet energy gap. Going back to Figure 1, along path II, the energy gap just described is decomposed into two contributions, one at constant external potential, ΔE_v, (fixed geometry), and another at constant multiplicity, ΔE_{N_S}. Thus, one can write that

$$\Delta E_{ST}^{ad} = \Delta E_v + \Delta E_{N_S} \quad (4)$$

where, according to eq 2, each contribution is given by

$$\Delta E_v = 2\mu_S^{(S)} + 2\eta_{SS}^{(S)} \quad (5)$$

$$\Delta E_{N_S} = \int d\mathbf{r}\, \rho^{(T/S)}(\mathbf{r})\, \Delta v(\mathbf{r}) + {}^1/_2 \int\int d\mathbf{r}\, d\mathbf{r}'\, \chi^{(T/S)}(\mathbf{r},\mathbf{r}')\, \Delta v(\mathbf{r})\, \Delta v(\mathbf{r}') \quad (6)$$

where the superscripts (T/S) denote that these coefficients are evaluated for the triplet at the external potential corresponding to the singlet.

Both paths are equivalent, but path II requires the following steps: (1) geometry optimization of the singlet state, (2) single-point calculation with a multiplicity of 3, fixing the geometry to that obtained in the previous step, and (3) geometry optimization of the triplet state taking the initial geometry as that corresponding to the singlet. By defining the reference in this manner, path II corresponds to the physical process of a vertical excitation from the singlet to the triplet followed by the relaxation to the triplet ground-state geometry. Thus, changes at constant external potential represent vertical excitations or decay processes, and changes at constant spin number (multiplicity) are geometry relaxations.

There is an underlying assumption in the above derivation. It has been assumed that the energy and its partial and functional derivatives are continuous. Maintaining this assumption and recalling that the expressions derived by Galván et al. for the spin potential,[1,2] in terms of the Kohn−Sham spin-polarized frontier eigenenergies, depend on whether one is increasing or decreasing the number of unpaired electrons, one can rewrite eq 5 in a more precise way as

$$\Delta E_v = 2\mu_S^{(S)+} + 2\eta_{SS}^{(S)} \quad (7)$$

where $\mu_S^{(S)+}$ is the spin potential of the singlet in the direction where N_S increases, i.e., on going from the singlet to the triplet. Certainly, spin symmetry imposes the restriction

$$\mu_S^{(S)-} = -\mu_S^{(S)+} \quad (8)$$

This latter fact, together with the numerical evidence that has been presented by Galván and Vargas,[2] suggests that the dependence of the energy on N_S is continuous but has noncontinuous first partial derivatives with respect to the spin number evaluated at even values of N_S, when the total number of electrons is also even. This conjecture is schematically depicted in Figure 2. This figure shows that the $E(N_S)$ curve is a piecewise continuous function with first partial derivatives that are discontinuous when the number of unpaired electrons is even and the total number of electrons is kept fixed.

Now, to evaluate eq 7, one needs an expression for the spin hardness, $\eta_{SS}^{(S)}$, that can be naively obtained in the following

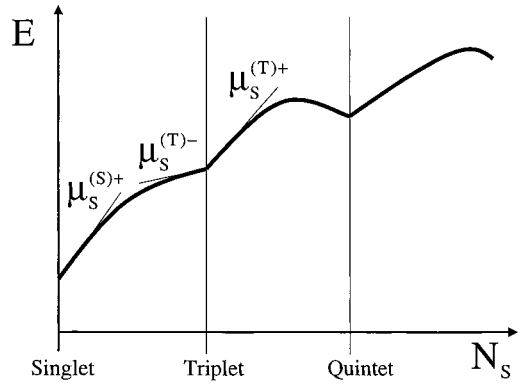

Figure 2. Schematic dependence of the total energy of an electronic system with an even number of electrons and as a function of the number of unpaired electrons (N_S), when the total number of electrons (N) and the external potential ($v(\mathbf{r})$) are constant.

way. Since

$$\eta_{SS} = \left(\frac{\partial^2 E}{\partial N_S^2}\right)_{N,v(\mathbf{r})} = \left(\frac{\partial \mu_S}{\partial N_S}\right)_{N,v(\mathbf{r})} \quad (9)$$

the finite differences approximation of the last derivative in eq 9 is given by

$$\eta_{SS} \cong \frac{\mu_S^{(T)-} - \mu_S^{(S)+}}{2} \quad (10)$$

where $\mu_S^{(T)-}$ is the spin potential of the triplet evaluated in the direction of decreasing multiplicity, i.e., toward the singlet. Substituting this latter equation into eq 7, one has

$$\Delta E_v = \mu_S^{(S)+} + \mu_S^{(T)-} \quad (11)$$

Using the expressions derived by Galván et al.[1,2] for μ_S^+ and μ_S^-,

$$\mu_S^+ = {}^1/_2(\epsilon_{LUMO\uparrow} - \epsilon_{HOMO\downarrow}), \quad \text{when } N_S \text{ increases} \quad (12)$$

$$\mu_S^- = {}^1/_2(\epsilon_{HOMO\uparrow} - \epsilon_{LUMO\downarrow}), \quad \text{when } N_S \text{ decreases} \quad (13)$$

where $\epsilon_{HOMO\sigma}$ and $\epsilon_{LUMO\sigma}$ are the orbital energies of the highest occupied and lowest unoccupied molecular spin−orbitals with spin σ, respectively, one obtains expressions that allow the calculation of the vertical singlet−triplet gap solely in terms of the frontier spin−orbital energies.

The previous derivation can be seriously objected to because it relies on the erroneous assumption of analyticity of the $E(N_S)$ function. However, by taking into consideration the facts provided by the numerical evidence, and by assuming that the piecewise continuous $E(N_S)$ function is a polynomial of degree 2 in the open interval $N_S \in (0,2)$, it can be shown that the same expressions for the spin hardness (eq 10) and the vertical singlet−triplet energy gap (eq 11) are recovered. It is worth noting that η_{SS} measures the concavity of the E versus N_S curve in this interval. Values of η_{SS} for the halocarbenes with different approximations to the exchange-correlation energy functional are presented in Table 1. They provide further evidence, in molecules, about the conjectured structure depicted in Figure 2 for the behavior of the energy as a function of the number of unpaired electrons. Thus, the simplicity of the expression for calculating the vertical singlet−triplet gap in terms of the spin-dependent response functions is the same, when one derives it by taking into account the conjectured form of the $E(N_S)$ function or using naively the finite differences approximation for the spin hardness.

TABLE 1: Spin Hardness for the Halocarbenes CXY (X, Y = H, F, Cl, Br, I), Calculated with Different Exchange-Correlation Energy Functionals[a]

	η_{SS} (eq 10)		
CXY	VWN	BPW91	B3PW91
CHF	−29.09	−51.07	−162.30
CHCl	−24.10	−43.43	−144.42
CHBr	−22.31	−39.77	−137.00
CHI	−76.76	−35.06	−68.585
CF_2	−36.32	−59.32	−174.00
CFCl	−28.44	−47.13	−151.57
CFBr	−25.14	−40.89	−140.93
CFI	−20.33	−32.94	−126.33
CCl_2	−23.24	−39.67	−135.78
CClBr	−21.52	−36.18	−128.91
CClI	−18.90	−31.51	−119.23
CBr_2	−19.99	−33.32	−122.68
CBrI	−17.63	−29.48	−114.40
CI_2	−15.86	−26.49	−107.13

[a] All values are in kJ/(mol·electron^2). For computational details, see the Appendix.

III. Results and Discussion

To test the validity of the theory developed in the previous section, results are presented for two approximations that allow the calculation of the vertical singlet−triplet energy gap in terms of the global spin-dependent response coefficients for halocarbenes.

A first order approximation is considered, where one keeps only the first term on the right hand side of eq 7. Using eq 12 for the spin potential of the singlet state leads one to the following approximate expression for the vertical singlet−triplet gap:

$$\Delta E_{ST}^{VERTICAL} \approx \Delta E_v^{(1)} = 2\mu_S^{(S)+} \cong \epsilon_{LUMO}^S - \epsilon_{HOMO}^S \quad (14)$$

where the spin dependence has been dropped due to the fact that for a singlet state the α and β orbital energies of the HOMO (and LUMO) are equal. Thus, one recovers the well-known expression derived within the context of unrestricted Hartree−Fock theory[37] that relates the vertical singlet−triplet energy gap to the difference between the LUMO and HOMO of the singlet state. Consequently, one also obtains and justifies the rule stating that large HOMO−LUMO gaps of the singlet stabilize this state with respect to the triplet.

In Figure 3, results for the vertical singlet−triplet energy gap for the halocarbenes, calculated within Kohn−Sham theory with several approximations to the exchange-correlation energy functional (see Appendix for computational details), are depicted. It can be seen that, independently of the theoretical level used, the spin potential goes practically parallel to $\Delta E_{ST}^{VERTICAL}$. The relation established by eq 14 is further tested in Figure 4. The slopes and correlation coefficients of the least squares linear fits (dashed lines in Figure 4) are 0.908 and 0.995 for the local (VWN), 0.856 and 0.938 for the semilocal (BPW91), and 0.656 and 0.938 for the hybrid (B3PW91) functionals, respectively. In all cases, this first order approximation overestimates the vertical singlet−triplet energy difference, but the linear relation between $\Delta E_{ST}^{VERTICAL}$ and the spin potential of the singlet state ($\mu_S^{(S)+}$) is satisfied. The agreement is better for the local and semilocal approximations, while it is less satisfactory for the hybrid, not only because of

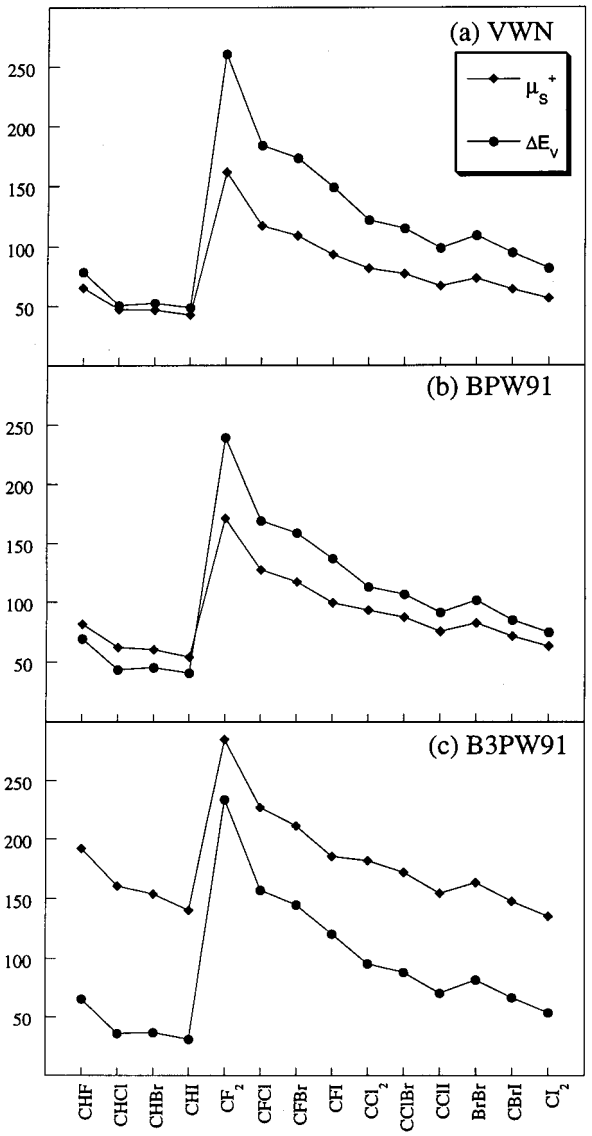

Figure 3. Vertical singlet−triplet energy gaps and spin potentials of the singlet state for the halocarbenes CXY (X, Y = H, F, Cl, Br, and I), calculated at (a) local (VWN), (b) semilocal (BPW91), and (c) hybrid (B3PW91) levels within Kohn−Sham theory. Energies are in kilojoules per mole and spin potentials in kilojoules per (mole−electron).

deviations from linearity but also because the overestimation is more pronounced. The enhanced HOMO−LUMO gap produced by including Hartree−Fock exchange in this latter functional is the main reason for the overestimation of $\Delta E_{ST}^{VERTICAL}$. This fact can also be appreciated in Figure 3. For all of the halocarbenes tested, and in contrast to VWN and BPW91, the hybrid HOMO−LUMO gap always goes above $\Delta E_{ST}^{VERTICAL}$.

As shown in section II, eq 11 is a first order approximation from the transition-state point of view, but considering the singlet (or triplet) state as the reference point, it can also be interpreted as including second order effects. Thus, the second approach, which will be called a second order approximation, is obtained upon substituting eqs 12 and 13 in eq 11. This procedure leads to

$$\Delta E_{ST}^{VERTICAL} \cong \Delta E^{(2)}{}_{v} = \mu_S^{(S)+} + \mu_S^{(T)-}$$

$$\cong {}^1/_2(\epsilon_{LUMO}^S - \epsilon_{HOMO}^S + \epsilon_{HOMO\uparrow}^T - \epsilon_{LUMO\downarrow}^T) \qquad (15)$$

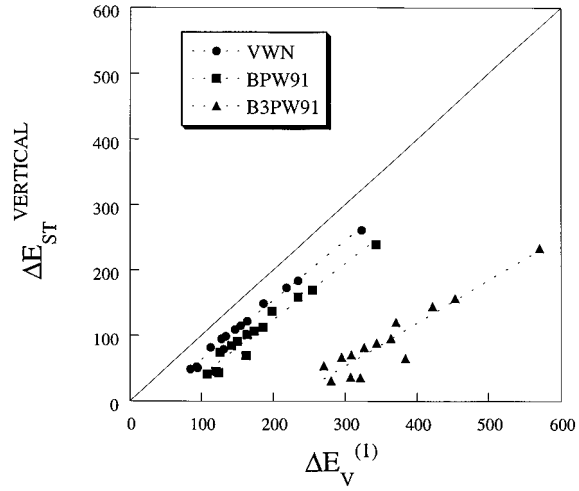

Figure 4. Exact versus first order approximation (eq 14) to the vertical singlet−triplet energy gap of the halocarbenes CXY (X, Y = H, F, Cl, Br, and I), calculated at local (VWN), semilocal (BPW91), and hybrid (B3PW91) levels within Kohn−Sham theory. Both quantities are in kilojoules per mole.

TABLE 2: Spin Potentials for the Singlet ($\mu_S^{(S)+}$) and Triplet ($\mu_S^{(T)-}$) of the Halocarbenes CXY (X, Y = H, F, Cl, Br, I), Calculated with Different Exchange-Correlation Energy Functionals[a]

	$\mu_S^{(S)+}$			$\mu_S^{(T)-}$		
CXY	VWN	BPW91	B3PW91	VWN	BPW91	B3PW91
CHF	65.61	81.29	191.88	7.43	−20.85	−132.72
CHCl	47.31	62.11	160.58	−0.89	−24.76	−128.26
CHBr	46.75	60.19	153.85	2.13	−19.35	−120.14
CHI	42.48	54.05	140.35	−111.00	−16.07	3.18
CF_2	161.52	171.43	285.17	88.87	52.80	−62.83
CFCl	117.16	127.31	226.79	60.28	33.06	−76.35
CFBr	109.09	117.12	210.92	58.81	35.34	−70.94
CFI	93.36	99.18	185.15	52.69	33.29	−67.50
CCl_2	82.01	92.86	181.65	35.52	13.52	−89.92
CClBr	77.43	86.90	171.80	34.39	14.55	−86.01
CClI	67.15	75.23	154.34	29.35	12.21	−84.12
CBr_2	73.62	82.07	163.21	33.63	15.44	−82.15
CBrI	64.22	71.16	147.59	28.96	12.21	−81.21
CI_2	56.50	62.99	135.29	24.78	10.00	−78.98

[a] All values are in kJ/(mol·electron). For computational details, see the Appendix.

An interesting feature of this expression is that since $\mu_S^{(T)-}$ is strictly less than $\mu_S^{(S)+}$ (see Table 2), the predicted second order vertical singlet−triplet gap will be smaller than $2\mu_S^{(S)+}$, correcting in the right direction the overestimation obtained with $\Delta E_v^{(1)}$. The comparison between the values predicted by eq 15 with the exact vertical singlet−triplet gap of halocarbenes is shown in Figure 5. The slopes and correlation coefficients of the least squares linear fits (dashed lines in Figure 5) are 0.984 and 1.0 for the local (VWN), 0.998 and 0.999 for the semilocal (BPW91), and 1.0 and 0.999 for the hybrid (B3PW91) functionals. One should notice the considerable improvement obtained for the hybrid functional, which results from the fact that, contrary to VWN and BPW91, the spin potential for the triplet is always negative (see Table 2). Thus, one can conclude that, independently of the level of theory used to study these vertical excitations in halocarbenes, the relation between the energy gaps and the frontier spin−orbital energies established by eq 15 holds in general for these systems.

No model for the geometry relaxation will be presented in this work. However, it is worth noting that for the systems tested here there is a linear relation between the adiabatic and

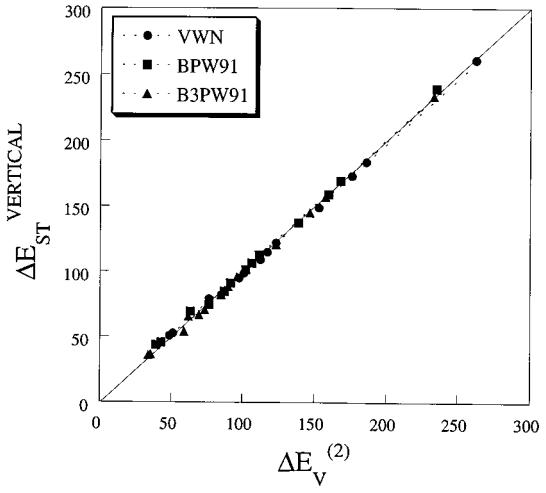

Figure 5. Exact versus second order approximation (eq 15) to the vertical singlet−triplet energy gap of the halocarbenes CXY (X, Y = H, F, Cl, Br, and I), calculated at local (VWN), semilocal (BPW91), and hybrid (B3PW91) levels within Kohn−Sham theory. Both quantities are in kilojoules per mole.

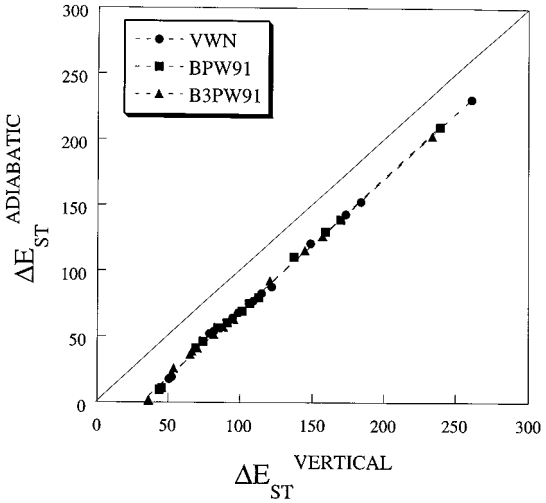

Figure 6. Adiabatic versus vertical singlet−triplet energy gaps of the halocarbenes CXY (X, Y = H, F, Cl, Br, and I), calculated at local (VWN), semilocal (BPW91), and hybrid (B3PW91) levels within Kohn−Sham theory. Both quantities are in kilojoules per mole.

vertical singlet−triplet energy differences. This fact can be appreciated in Figure 6. Again, the linearity holds for the three exchange correlation functionals. This result implies that the energy contribution to the adiabatic gap due to the geometrical relaxation in halocarbenes is almost constant. Since it has been previously shown that the vertical energy is proportional to the spin potential, the linear relation between the adiabatic and vertical singlet−triplet energies leads one to conclude that the former excitation energy in halocarbenes is also linearly related to the spin potential.

IV. Conclusions

The spin-polarized extension of density functional theory is used to demonstrate that the vertical singlet−triplet energy difference is linearly related to the global spin-dependent response coefficients. For the halocarbenes CXY (X, Y = H, F, Cl, Br, and I), Kohn−Sham calculations with different exchange correlation energy functionals show that this relation holds, idependently of the level of theory used. A first order approximation overestimates these gaps, particularly for the hybrid functionals, and the inclusion of spin hardness through a transition-state-like approach considerably improves the predicted vertical singlet−triplet gaps.It is also shown that for halocarbenes there is a linear relation between the adiabatic and vertical singlet−triplet gaps that together with the previous conclusion implies the existence of a linear relation between the geometrical relaxation energy and the spin potential. A deeper analysis of this fact is required, and it is currently being investigated in our laboratory.

In summary, the present work shows that the global spin-dependent response coefficients are useful in describing important aspects of chemical reactivity that cannot be described within the spin restricted version of the theory.

TABLE 3: Basis Sets and Contraction Schemes for the Atoms in the Halocarbenes Studied in the Present Work[a]

atom	basis set	contraction
C	DZVP	(621/41/1*)
F	DZVP	(621/41/1*)
Cl	DZVP	(6321/521/1*)
Br	DZVP	(63321/5321/41+)
I	DZVP	(633321/53321/531*)
H	DZVPP	(41/1*)

[a] Exponents and coefficients from ref 39.

TABLE 4: Optimized Bond Distances for the Halocarbenes CXY (X, Y = H, F, Cl, Br, I), Calculated with Different Exchange-Correlation Energy Functionals[a]

		LSDA		BPW91		B3PW91	
	C−X	$^1A_1$	$^3B_1$	$^1A_1$	$^3B_1$	$^1A_1$	$^3B_1$
CHF	C−H	1.142 (1.138)[a]	1.104	1.139	1.099	1.126	1.091
	C−F	1.314 (1.305)[b]	1.312	1.338	1.335	1.319	1.322
CHCl	C−H	1.129	1.099	1.127	1.095	1.115	1.088
	C−Cl	1.699	1.656	1.729	1.683	1.709	1.673
CHBr	C−H	1.128	1.099	1.127	1.096	1.114	1.088
	C−Br	1.858	1.807	1.893	1.838	1.872	1.827
CHI	C−H	1.128	1.099	1.127	1.096	1.115	1.089
	C−I	2.064	1.998	2.102	2.035	2.083	2.025
CF_2	C−F	1.311 (1.304)[a]	1.318	1.334	1.339	1.313	1.323
CFCl	C−F	1.307	1.317	1.329	1.338	1.308	1.323
	C−Cl	1.750	1.680	1.784	1.706	1.757	1.693
CFBr	C−F	1.302	1.314	1.322	1.335	1.303	1.320
	C−Br	1.933	1.841	1.975	1.874	1.944	1.857
CFI	C−F	1.299	1.312	1.319	1.333	1.300	1.318
	C−I	2.168	2.051	2.219	2.092	2.186	2.076
CCl_2	C−Cl	1.732 (1.716)[a]	1.674	1.762	1.700	1.735	1.686
CClBr	C−Cl	1.721	1.670	1.750	1.696	1.725	1.683
	C−Br	1.905	1.831	1.946	1.864	1.914	1.848
CClI	C−Cl	1.717	1.668	1.743	1.695	1.720	1.681
	C−I	2.133	2.033	2.182	2.072	2.147	2.057
CBr_2	C−Br	1.895 (1.740)[a]	1.827 (1.74)[b]	1.932	1.860	1.903	1.844
CBrI	C−Br	1.889	1.825	1.924	1.856	1.896	1.842
	C−I	2.119	2.027	2.158	2.070	2.130	2.053
CI_2	C−I	2.111	2.023	2.147	2.062	2.121	2.047

[a] All values are in angstroms. [b] Experimental values taken from the following references: CHF, ref 12; CCl_2, ref 15; CF_2, ref 9; CBr_2, ref 10.

Acknowledgment. We would like to acknowledge fruitful discussions with Dr. Jorge Garza and Dr. Andrés Cedillo. Computer time was provided by the Laboratorio de Cómputo Paralelo y Visualización at UAM-Iztapalapa. R.V. acknowledges support provided by a CONACYT scholarship.

TABLE 5: Optimized Bond Angles for the Halocarbenes CXY (X, Y = H, F, Cl, Br, I), Calculated with Different Exchange-Correlation Energy Functionals[a]

	LSDA		BPW91		B3PW91	
	$^1A_1$	$^3B_1$	$^1A_1$	$^3B_1$	$^1A_1$	$^3B_1$
CHF	101.3 (104.1)[b]	120.7	101.1	120.6	101.6	120.9
CHCl	101.6	126.1	101.1	125.5	101.9	125.8
CHBr	101.2	126.2	99.7	125.9	100.6	126.2
CHI	99.6	128.2	99.4	127.8	100.2	128.4
CF_2	104.1 (104.8)[b]	119.3	104.1	119.8	104.3	119.5
CFCl	105.9	122.9	106.1	123.1	106.2	122.9
CFBr	106.1	123.7	106.4	124.0	106.4	123.7
CFI	107.2	125.1	107.4	125.2	107.4	124.9
CCl_2	109.2 (109.2)[b]	128.2	109.4	128.1	109.6	130.5
CClBr	109.4	128.9	109.7	128.8	109.8	129.3
CClI	110.6	130.7	110.9	130.7	111.0	130.9
CBr_2	109.4 (∼114)[b]	129.2 (∼150)[b]	109.9	129.4	110.0	129.3
CBrI	110.6	130.9	111.3	131.1	111.2	130.9
CI_2	111.6	132.7	112.1	132.7	112.2	132.9

[a] All values are in degrees. [b] Experimental values taken from the following references: CHF, ref 12; CCl_2, ref 15; CF_2, ref 9; CBr_2, ref 10.

TABLE 6: Adiabatic Singlet−Triplet Energy Differences for the Halocarbenes CXY (X, Y = H, F, Cl, Br, I), Calculated with Different Exchange-Correlation Energy Functionals[i]

CXY	LSDA	BPW91	B3PW91	exptl or previous works
CH_2	−57.61	−68.33	−68.99	−38.12[a] −50.21[b] −37.66[c,d]
CHF	51.92	41.00	36.15	47.28[a] 48.12[d] 53.97[e]
CHCl	17.78	9.62	1.30	
CHBr	19.25	10.88	1.30	
CHI	14.10	6.40	−6.40	15.46[f]
CF_2	230.70	209.70	202.71	236.81[a] 233.47[g] 240.58[b]
CFCl	152.50	138.78	126.11	179.20[g] 164.85[h]
CFBr	142.90	129.49	115.39	
CFI	120.50	110.25	92.30	
CCl_2	87.65	79.50	62.97	91.67[g] 108.37[c]
CClBr	82.68	74.98	57.03	
CClI	67.95	60.25	41.05	
CBr_2	76.90	69.25	51.30	87.40[g] 93.72[g]
CBrI	64.10	56.40	38.45	
CI_2	53.85	46.15	25.65	65.81[g] 64.02[d]

[a] Experimental values taken from the following references: CHF (ref 14); CH_2 (ref 13) and CF_2 (ref 11). [b] ref 19; [c] ref 20, [d] ref 25, [e] ref 17, [f] ref 28, [g] ref 22, [h] ref 18 [i] All values are in kilojoules per mol.

Appendix

All calculations reported in this work solve the Kohn−Sham equations within the linear combination of Gaussian-type orbitals (LCGTO) as implemented in Gaussian 94.[38] Basis sets for C, H, F, Cl, Br, and I were taken from Godbout et al.;[39] the contraction schemes for each atom are shown in Table 3. All integrations were done numerically with a fine-pruned grid.[40] To analyze the effect of density inhomogenities and the role of Hartree−Fock exchange in the calculation of the spin potential and spin hardness of halocarbenes, the following approximations to the exchange-correlation energy functional were tested: a local functional using Vosko, Wilk, and Nusair's (VWN) parametrization,[41] a semilocal (generalized gradient approximation) using Becke's exchange and Perdew and Wang correlation (BPW91),[42] and a three-parameter hybrid functional (B3PW91) with the same exchange and correlation as those in the semilocal one.[43] The semilocal and hybrid approximations were incorporated self-consistently in the solution of Kohn−Sham equations. Full geometry optimizations using Berny's gradient method[44] were done for the singlet and triplet states of all halocarbenes. Optimized and available experimental bond distances and bond angles are reported in Tables 4 and 5. In agreement with previous calculations, the local functional provides the best bond distances when compared with available experimental information. Bond angles are less sensitive to the exchange-correlation energy functional, and in all cases, for all functionals, the bond angle in the triplet ($^3B_1$) state is larger than in the singlet ($^1A_1$) state. In general, the most important geometrical effect of the singlet−triplet excitation of halocarbenes is on bond angles, which always increase. Bond distances are less affected, and there is no unique trend for all halocarbenes.

The adiabatic singlet−triplet energy differences calculated at local, semilocal, and hybrid levels, together with available experimental values as well as other theoretical predictions, are reported in Table 6. As expected, the local approximation

TABLE 7: ZPE Corrected Adiabatic Singlet−Triplet Energy Differences for the Halocarbenes CXY (X, Y = H, F, Cl, Br, I), Calculated with Different Exchange-Correlation Energy Functionals[a]

CXY	LSDA	BPW91	B3PW91
CHF	52.51	41.71	36.48
CHCl	18.45	10.46	1.80
CHBr	20.13	11.72	1.46
CHI	14.85	8.79	−6.07
CF_2	230.7	209.79	202.55
CFCl	153.2	139.54	126.52
CFBr	143.9	130.21	115.98
CFI	121.5	111.50	92.38
CCl_2	89.12	80.67	63.81
CClBr	83.55	75.81	57.91
CClI	70.67	61.71	42.72
CBr_2	77.74	70.29	52.30
CBrI	65.23	57.32	38.20
CI_2	54.22	46.48	25.40

[a] All values are in kilojoules per mole.

TABLE 8: Vertical Singlet−Triplet Energy Differences for the Halocarbenes CXY (X, Y = H, F, Cl, Br, I), Calculated with Different Exchange-Correlation Energy Functionals[a]

CXY	LSDA	BPW91	B3PW91
CH_2	−9.67	−19.75	−22.64
CHF	78.99	69.29	65.40
CHCl	50.63	43.68	35.90
CHBr	52.55	45.52	36.53
CHI	48.70	40.96	30.75
CF_2	260.90	239.32	233.63
CFCl	183.80	169.37	157.03
CFBr	173.10	158.95	144.85
CFI	148.70	137.19	120.50
CCl_2	121.80	112.68	95.69
CClBr	114.70	106.40	88.45
CClI	98.70	91.04	70.50
CBr_2	109.00	101.29	82.05
CBrI	94.85	84.60	66.65
CI_2	82.05	74.35	53.85

[a] All values are in kilojoules per mole.

provides the largest adiabatic gap followed by the semilocal and hybrid functionals. However, this reduction on the ground state energies of these systems for BPW91 and B3PW91 provides results that deviate more from experiment or high-quality ab initio calculations. The hybrid adiabatic gaps predicted for these molecular systems are too small, indicating the inability of this model exchange-correlation functional to properly describe these excitation energies. It is worth noting that, according to the calculations reported in this work, there is only one system, CHI, where different functionals predict different ground states. For CHI, local and semilocal calculations predict the singlet ($^1A_1$) to be the ground state, which is in agreement with previous calculations, while the hybrid predicts the triplet, $^3B_1$, as the ground state. Harmonic frequencies were also calculated to estimate the zero point energy (ZPE) correction. The ZPE corrected adiabatic energy gaps are reported in Table 7. By comparing Tables 6 and 7, it is found that the ZPE correction is small; the largest ZPE correction is 2.72 kJ/mol for CClI. It is worth noting that this correction does not solve the controversial ground-state assignment of CHI. Single point calculations for the triplet at the optimized geometry of the singlet were also done to calculate the vertical singlet−triplet energy gap. The calculated values are reported in Table 8 for the three theoretical models considered in this work. The orbital energies of these single point calculations are those used to calculate the quantity $\mu_S^{(T)-}$ introduced in the main text.

References and Notes

(1) Galván, M.; Vela, A.; Gázquez, J. L. *J. Phys. Chem.* **1988**, *92*, 6470.
(2) Galván, M.; Vargas, R. *J. Phys. Chem.* **1992**, *96*, 1625.
(3) Vargas, R.; Galván, M. *J. Phys. Chem.* **1996**, *100*, 14651.
(4) Ghanty, T. K.; Ghosh, S. K. *J. Phys. Chem.* **1991**, *95*, 6512.
(5) Ghanty, T. K.; Ghosh, S. K. *Inorg. Chem.* **1992**, *31*, 1951.
(6) Ghanty, T. K.; Ghosh, S. K. *J. Phys. Chem.* **1994**, *98*, 1840.
(7) Ghanty, T. K.; Ghosh, S. K. *J. Phys. Chem.* **1994**, *98*, 9197.
(8) Ghanty, T. K.; Ghosh, S. K. *J. Am. Chem. Soc.* **1994**, *116*, 8801.
(9) Mathews, C. W. *Can. J. Phys.* **1967**, *45*, 2355.
(10) Ivery, R. C.; Schultze, P. D.; Leggett, T. L.; Kohl, D. A. *J. Chem. Phys.* **1974**, *60*, 3174.
(11) Koda, S. *Chem. Phys. Lett.* **1978**, *55*, 353.
(12) Susuki, T.; Saito, S.; Hirota, J. *J. Mol. Spectrosc.* **1981**, *90*, 447.
(13) McKellar, A. R. W.; Bunker, P. R.; Sears, T. J.; Evenson, K. M.; Saykally, R. J.; Langhoff, S. R. *J. Chem. Phys.* **1983**, *79*, 5251.
(14) Murray, K. K.; Leopold D. G.; Miller T. M.; Lineberger, W. C. *J. Chem. Phys.* **1988**, *89*, 4442.
(15) Mujikate, M.; Hirota, E. *J. Chem. Phys.* **1989**, *91*, 3426.
(16) Bauschlicher, C. W.; Schaefer, H. F., III; Bagus, P. S. *J. Am. Chem. Soc.* **1977**, *99*, 7106.
(17) Luke, B. T.; Pople, J. A.; Krogh-Jespersen, M. B.; Apeloig, Y.; Karni, M.; Chaudrasekhar, J.; von Rague Schleyer, P. *J. Am. Chem. Soc.* **1980**, *102*, 764.
(18) Carter, E. A.; Goddard, W. A., III. *J. Phys. Chem.* **1986**, *90*, 998.
(19) Bauschlicher, C. W., Jr.; Taylor, P. R. *J. Chem. Phys.* **1986**, *85*, 5936.
(20) Carter, E. A.; Goddard, W. A., III. *J. Phys. Chem.* **1987**, *91*, 4651.
(21) Carter, E. A.; Goddard, W. A., III. *J. Chem. Phys.* **1988**, *88*, 1752.
(22) Gutzev, G. L.; Ziegler, T. *J. Phys. Chem.* **1991**, *95*, 7220.
(23) Kim, S.; Hamilton, T. P.; Schaefer, H. F., III. *J. Chem. Phys.* **1991**, *94*, 2063.
(24) Irikura, K. K.; Goddard, W. A., III; Beauchamp, J. L. *J. Am. Chem. Soc.* **1992**, *114*, 48.
(25) Russo, N.; Sicilia, E.; Toscano, M. *J. Chem. Phys.* **1992**, *97*, 5031.
(26) Clauberg, H.; Minsek, D. W.; Chen, P. *J. Am. Chem. Soc.* **1992**, *114*, 99.
(27) Nash, J. J.; Dowd, P.; Jordan, K. D. *J. Am. Chem. Soc.* **1992**, *114*, 10072.
(28) Russo, N.; Sicilia, E.; Toscano, M. *Chem. Phys. Lett.* **1993**, *213*, 245.
(29) Khodabandeh, S.; Carter, E. A. *J. Phys. Chem.* **1993**, *97*, 4360.
(30) Matzinger, S.; Fulscher, M. P. *J. Phys. Chem.* **1995**, *99*, 10747.
(31) García, V. M.; Castell, O.; Reguero, M.; Caballol, R. *Mol. Phys.* **1996**, *87*, 1395.
(32) Tomioka, H. *Acc. Chem. Res.* **1997**, *30*, 315.
(33) Berson, J. A. *Acc. Chem. Res.* **1997**, *30*, 2239.
(34) Kirmse, W. *Carbene Chemistry;* Academic: New York, 1971.
(35) Pross, A. *Theoretical & Physical Principles of Organic Reactivity*; Wiley: New York, 1995.
(36) Schuster, G. B. *Adv. Phys. Org. Chem.* **1986**, *22*, 311.
(37) Hatfield, W. E. In *Magneto-Structural Correlations in Exchange Coupled Systems;* Willet, R. D., Gatteschi, D., Kohn, O., Eds.; Reidel: Amsterdam, 1985; p 555.
(38) Frisch, M. J.; Trucks, G. W.; Schlegel, H. B.; Gill, P. M. W.; Johnson, B. G.; Robb, M. A.; Cheeseman, J. R.; Keith, T. A.; Petersson, G. A.; Montgomery, J. A.; Raghavachari, K.; Al-Laham, M. A.; Zakrzewski, V. G.; Ortiz, J. V.; Foresman, J. B.; Ciolowski, J.; Stefanov, B. B.; Nanayakkara, A.; Challacombe, M.; Peng, C. Y.; Ayala, P. Y.; Chen, W.; Wong, M. W.; Andres, J. L.; Replogle, E. S.; Gomperts, R.; Martin R. L.; Fox, D. J.; Binkley, J. S.; Defrees, D. J.; Baker, J.; Stewart, J. P.; Head-Gordon, M.; Gonzalez, C.; Pople, J. A. *Gaussian 94*; Gaussian: Pittsburgh, PA, 1995.
(39) Godbout, N.; Salahub, D. R.; Andzelm, J.; Wimmer, E. *Can. J. Phys.* **1992**, *70*, 560.
(40) Trucks, G. W.; Frisch, M. J. *Rotational invariance properties of pruned grids for numerical integration*. Manuscript in preparation.
(41) Vosko, S. H.; Wilk, L.; Nusair, M. *Can. J. Phys.* **1980**, *58*, 1200.
(42) (a) Becke, A. D. *Phys. Rev. A* **1988**, *38*, 3098. (b) Perdew, J. P.; Wang, Y. *Phys. Rev. B* **1992**, *45*, 13244.
(43) Becke, A. D. *J. Chem. Phys.* **1993**, *98*, 5648.
(44) Schlegel, H. B. *J. Comput. Chem.* **1982**, *3*, 214.